Desalination 414 (2017) 10–17

Contents lists available at ScienceDirect

Desalination

journal homepage: www.elsevier.com/locate/desal

Fabrication of super-hydrophobic polypropylene hollow fiber membrane and its application in membrane distillation

Zhihao Xu [a,b], Zhen Liu [a,b,*], Pengfei Song [a,b], Changfa Xiao [a,b]

[a] State Key Laboratory of Separation Membranes and Membrane Processes, Tianjin Polytechnic University, Tianjin 300387, China
[b] School of Materials Science and Engineering, Tianjin Polytechnic University, Tianjin 300387, China

HIGHLIGHTS

- Silica particles are attached to membrane surface, in order to increase the roughness.
- Hollow fiber membrane is modified by 1H, 1H, 2H, 2Hperfluorooctyltriethoxysilane to reduced surface free energy.
- Salt flux of the polypropylene super-hydrophobic membrane is almost same as the untreated membranes.
- The retention rate of the modified membrane is improved.

GRAPHICAL ABSTRACT

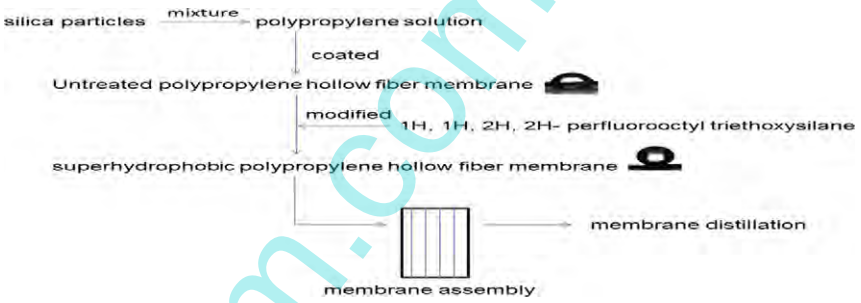

ARTICLE INFO

Article history:
Received 22 September 2016
Accepted 22 March 2017
Available online xxxx

Keywords:
Super-hydrophobicity
Polypropylene hollow fiber membrane
Silica particles
Polypropylene particles
Membrane distillation

ABSTRACT

The main aim of the current study is to prepare super-hydrophobic polypropylene hollow fiber membranes. However, polypropylene hollow fiber membrane surface is very smooth and difficult to attach silica particles. To solve this problem, a method including combined use of silica particles and polypropylene solution is used to preparation the super-hydrophobic coatings. The collosol mixed by the silica particles and PP particles were coated to the membrane surface. Then the membrane was modified by 1H,1H,2H,2H-Perfluorooctyltriethoxysilane (POTS) that exhibited a super-hydrophobic surface with a static water contact angle of 157°. Surface elemental analyses of membrane were characterized by XPS and surface analyses (FT-IR, FESEM, AFM, contact angle measurements and MIP). In addition, membrane distillation experiments of NaCl solutions were carried out in unmodified and modified polypropylene hollow fiber membrane. The results indicated that, compared with the untreated membranes, the modified membranes had higher flux and rejection.

1. Introduction

Super-hydrophobic surfaces can be seen everywhere in daily life: Lotus leaf [1] surface is micro and nano structure which has a self-cleaning function; water strider's [2] legs have different scales of surface roughness which can float in the water to produce super-hydrophobicity; raindrops are falling from butterfly wings [3], etc. In recent years, the super-hydrophobic surface has attracted more and more attention and research [4–7]. Meanwhile, it has been widely used in ice-phobicity [8], corrosion [9], anti-pollution [10], anti-oxidation [11], preventing current conduction [12] and self-purification [13] and so on. Super-hydrophobic surface means contact angle should be higher than 150° with a small roll angle. There are many ways to prepare of the super-hydrophobic surface including phase separation of polymer blends [14], laser etching [15], solvent evaporation [9], template method [16], sublimation method [17]. Sol-gel method can also increase the surface roughness [18–20]. However, there are some processes which are complicated and require large

* Corresponding author at: School of Material and Science Engineering, Tianjin Polytechnic University, Tianjin 300387, China.
E-mail address: poly1122@sina.com (Z. Liu).

http://dx.doi.org/10.1016/j.desal.2017.03.029
0011-9164/

human and material resources to fabricate super-hydrophobic hollow fiber membranes.

In 2004, Erbil [9] and his colleagues used inexpensive polypropylene (PP) to obtain super-hydrophobic film with phase separation method. Simultaneously, this simple and low-cost method for forming a super-hydrophobic coating was widely used. Based on their work, Yuexia Lv et al. [21] successfully obtained a super-hydrophobic membrane by PP solution that was deposited onto PP hollow fiber membranes, and the modified fiber membranes were assembled in a membrane contactor to test film properties. Increasing the roughness of the coating can effectively increase the hydrophobicity of the coating, M. Yu et al. [22] applied a method which cotton fabrics were immersed in the silica sol, then the cotton fabrics were modified with a silane coupling agent in order to obtain a low surface energy coating, thereby the super-hydrophobic coating was prepared.

With the rapid development of science and technology and economy, the supply and demand of freshwater is increasing day by day. According to statistics, about 800 million people around the world cannot guarantee drinking water safety and about 1.1 billion people cannot use drinking water equipment. These figures represent a huge contradiction between fresh water demand and population. Therefore, how to alleviate the lack of fresh water is one of the problems the world needs to solve. Seawater desalination is one of the best sources of fresh water, and many membrane separation technologies have been applied in seawater desalination technology, such as multistage flash distillation (MSF), multiple-effect distillation (MED), sea water reverse osmosis (SWRO) or membrane distillation (MD). Among these technologies, membrane distillation (MD) has received a lot of attention because of its economy and easy operation. It is a great significance to solve the global shortage of fresh water for membrane distillation (MD).

Membrane distillation (MD) is a new non-isothermal membrane separation process. It is a thermally driven process that involves transport of water vapor through micro-porous hydrophobic membrane [23]. The driving force of MD is supplied by the vapor pressure difference generated by temperature gradient imposed between the liquid/vapor interfaces [24]. There are many ways of membrane distillation, such as direct contact membrane distillation (DCMD), air gap membrane distillation (AGMD), sweeping gas membrane distillation (SGMD), and vacuum membrane distillation (VMD) [25] which DCMD is the most common kind of membrane distillation method. Simultaneously, DCMD has been used in the production of fresh water [26,27], in wastewater treatment and reuse [28,29] and in the food industry [30–32].

Membrane is one of the most important factors for a successful MD process [33]. The hydrophobic character of the membrane avoids liquid from entering into pores, thanks to the surface tension forces. Thus, liquid/vapor interfaces are created at the entrances of the membrane pores [34]. The super-hydrophobic membrane can effectively prevent the solution from wetting the membrane surface, so the effect of membrane distillation is better than non-hydrophobic membrane. Some hydrophobic membranes can be used for membrane distillation, for example polyethylene (PE) membranes have been used for membrane distillation. Jian Z. et al. [33] studied the effect of different commercially available TIPS-made PE membranes on membrane distillation. They investigate the effects of membrane physicochemical properties and MD operation parameters on permeation flux and energy efficiency.

In this article, the above three methods were reference, silica particles were innovatively added to the homogeneous solution of polypropylene and this solution was applied to a polypropylene hollow fiber membrane to further increase the polypropylene hollow fiber membrane surface roughness. In order to obtain excellent hydrophobicity, the polypropylene hollow fiber membrane was modified by perfluorinated silane. Finally super-hydrophobic polypropylene hollow fiber membrane was fabricated with a contact angle of 157°. This method is inexpensive and easy to obtain, meanwhile it has good super-hydrophobic properties. Furthermore, the super-hydrophobic PP hollow fiber membranes applied in vacuum membrane distillation (VMD) of NaCl solution. The fluxes of the polypropylene hollow fiber membrane before and after the modification were measured at different temperatures. This study aims to improve membrane flux and increases retention of the PP hollow fiber membrane.

2. Experimental and methods

2.1. Materials

The materials used in the experiments are shown in Table 1, and none of the drugs have been purified.

2.2. Preparation of silica powder

25 mL of methanol, 75 mL of 2-propanol, 21 mL of ammonia solution were added to three-necked flask, and a mixture of APS and TEOS in different ratios with a combined volume of 10 mL. The three APS/TEOS volume ratios used were 1/19, 1/9, and 1/4 [35]. The mixture was mechanically solution was magnetic stirring at 300 rpm for 6 h at 60 °C. And then the solution was allowed to stand in a beaker and cooled 12 h. After skimming the upper supernatant, it was heated in a drying oven for 24 h at 75 °C to obtain a powdery silica.

2.3. Preparation of super-hydrophobic polypropylene hollow fiber membranes

0.7 g PP granules were dissolved completely in 30 mL *p*-xylene [21] at 120 °C with magnetic stirring 300 rpm. After that, different amounts of nanosilica (0.5 wt%, 1 wt%, 1.5 wt%, 2 wt%) were dispersed in 30 mL *p*-xylene followed by addition of MEK (5 mL) and cyclohexanone(5 mL) into PP/nanosilica solution under stirring. Finally, a homogeneous sol was obtained. The thermo sol was coated onto the polypropylene hollow fiber membrane. Repeated coating five times with the middle one-minute intervals, the coating membrane was washed with ethanol to remove residual solution.

2.4. Surface modification by POTS

50 mL of ethanol, 1 mL of water, 0.5 mL 1H,1H,2H,2H-Perfluorooctyltriethoxysilane were added in a beaker, and heated at 60 °C water bath for 6 h to prepare a POTS solution. The coated film was subjected to modification in a POTS solution and then dried at room temperature for 24 h.

2.5. Characterization techniques

Contact angles were measured with deionized water on a Dataphysics JY-82 instrument at room temperature (20 °C). Each sample was measured at least 4 times with 5 μL of distilled water with the sessile drop method. Field emission scanning electron microscope (FE-SEM) was performed on a HITACHIS-4800 instrument (Hitachi, Japan) in high-vacuum mode operated at a 2 kV acceleration voltage. To avoid electric charging all samples were plated with gold particles [36]. The thickness of the gold layer is less than 10 nm. Transmission electron microscopy (TEM, H7650, Hitachi, Ltd., Japan) was used to characterize the size of the silica particles. A scan size of 4 μm × 4 μm Atomic force microscope (AFM) image was obtained with CSPM5500 at room temperature (20 °C), in tapping mode. Surface chemical characterizations were carried out by X-ray photoelectron spectroscopy (XPS) on a K-Aepna system with Al/KR radiation as the X-ray source. The organic and inorganic bonds of the membrane surface were studied by FTIR (TENSOR37, Germany BRUKER company). Mercury intrusion porosimetry (MIP) was measured by automatic mercury analyzer (US61M/IV-9500), which greatest pressure was 33,000 lbs (228 MPa).

Table 1
Experimental reagents.

Reagent name	Purity	Production company
Polypropylene (PP)	Fiber grade(SEETEC H5300, density = 0.9 g/cm3)	SK Global Chemical Company
P-xylene (99%)	Analytical grade	Tianjin standard technology companies
3-Aminopropyl triethoxysilane (APS)	Analytical grade	Shanghai Aladdin reagent (China) Co., Ltd.
Tetraethylorthosilicate (TEOS, 98%)	Analytical grade	Shanghai Aladdin reagent (China) Co., Ltd.
Cyclohexanone	Analytical grade	Shanghai Aladdin reagent (China) Co., Ltd.
Ammonia (NH3·H2O, 25%)	Analytical grade	Tianjin Sailing Chemical Reagent Co., Ltd
2-Butanone (MEK)	Analytical grade	Tianjin Sailing Chemical Reagent Co., Ltd
Ethanol (99.7%)	Analytical grade	Tianjin Sailing Chemical Reagent Co., Ltd
Isopropanol	Analytical grade	Tianjin Sailing Chemical Reagent Co., Ltd
1H,1H,2H,2H-Perfluorooctyltriethoxysilane (POTS, 97%)	Enterprise standards	Hubei Jusheng Technology Co., Ltd
Distilled water	/	Homemade in laboratory
Polypropylene (PP) hollow fiber membrane	Outer diameter:0.5 mm, inner diameter of 0.36 mm	Homemade in laboratory

2.6. Membrane distillation apparatus experimental and procedures

The sodium chloride was added to water to prepare a solution of 3.5 wt%. The solution was passed through a certain flow of the pump into the membrane modules operating VMD at different temperatures and a vacuum degree of 0.1 MPa. And then distilled water was collected and measured by conductivity (Fig. 1). The unmodified membrane and the modified membranes were measured, respectively.

3. Results and discussion

3.1. Characterization of silica particle size

The sizes of silica particles are different due to the different proportions of TEOS and APS. As the TEOS content decreases, some amine groups cannot graft to silica particles, and the silica particles become smaller. The amine groups to the silica particles can be modified by fluorosilane for future hydrophobicity. Three different size of the silica particles were determined by TEM (Fig. 2). Fig. 3 shows FT-IR images of the membranes.

The FT-IR spectra displayed an absorption peaks located at 779.5 cm^{-1}, which was assigned to stretch vibrations of the Si-C bonds of the siloxane components. The peak of the Si-O-Si was appeared at 1135.8 cm^{-1}. The peak at 1199.4 cm^{-1} and 1237.5 were due to C-F_3 and Si-CH_3, respectively (Fig. 3). This indicates that the silica particles and F element are grafted to the membrane surface, which improves the hydrophobicity of the membrane.

3.2. Film surface morphology and wettability

Surface wettability is examined by contact angle (CA) measurements, and the size of water drop is 5 μL. By field emission scanning electron microscope (FE-SEM) silica particles can be observed the rough surface of the film. Air between the water drops and the surface can increase the hydrophobicity of the membrane.

It can be seen from Fig. 4, for a 5 μL water droplet, the surface of unmodified membrane was smooth with a water static CA of 73° (Fig. 4A). Pure PP hollow fiber membrane surface is smooth and the contact area between the solid surfaces of the water droplets is relatively large, so the contact angle is relatively small. When the PP hollow fiber membrane was only modified by POTS grafting, no significant change was observed by SEM (Fig. 4B). The water static CA is 97° because the surface free energy of the membrane surface decreases. With the chemical incorporation of silica particles into the membrane, a rough surface structure has been conveniently generated. Surface morphology of the hollow fiber membrane has taken place different changes. There were a number of non-spherical particles or large particles, possibly due to the aggregation of smaller particles [35]. For Fig. 4C to E, as the APS/TEOS ratio increased, the silica particles became smaller, more and more particles adhered to the membrane. As a result, a rough and porous surface structure had been conveniently generated. Fig. 4C showed contact angle of water was only 147°. With the particles into the membrane surface, the surface density increased so that a water static CA was 153° (Fig. 4D), but some free particles were not connected to the membrane. For Fig. 4E, the particle area density was the highest among the samples, and the contact angle of water was 157°. There is more contact area between the water droplet and the air rather than the membrane surface. Therefore, the density and surface roughness of the membrane reaches highest and the contact angle is the largest. The difference in the contact angles can be attributed to the different rough surface structure of the modified membranes. In general, there are two reasons to reach the super-hydrophobicity: on one hand, the higher the area density of silica particles and roughness on the membrane surface, the higher the water contact angle. On the other hand, perfluoroalkyl compounds have very low surface free energy. After a perfluoroalkyl modification, the surface free energy of the polypropylene hollow fiber membrane decreases so that the hydrophobicity significantly increased.

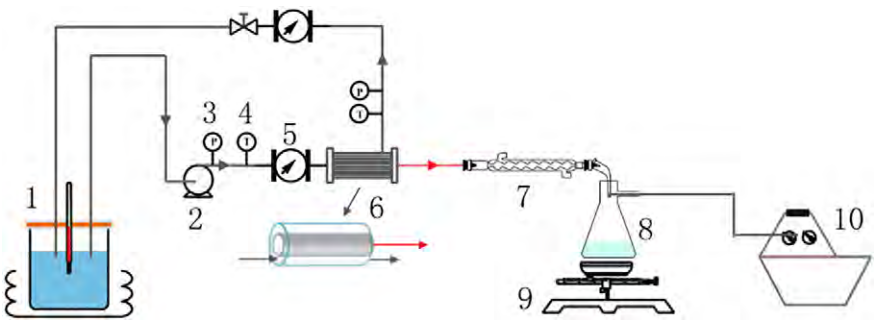

Fig. 1. Vacuum membrane distillation (VMD) flowchart. 1. thermostated feed tank, 2. water-pump, 3. pressure gauge, 4. thermometer, 5. flowmeter, 6. membrane module, 7. condensing tube, 8. permeate collection bottle, 9. balance, 10. vacuum pump.

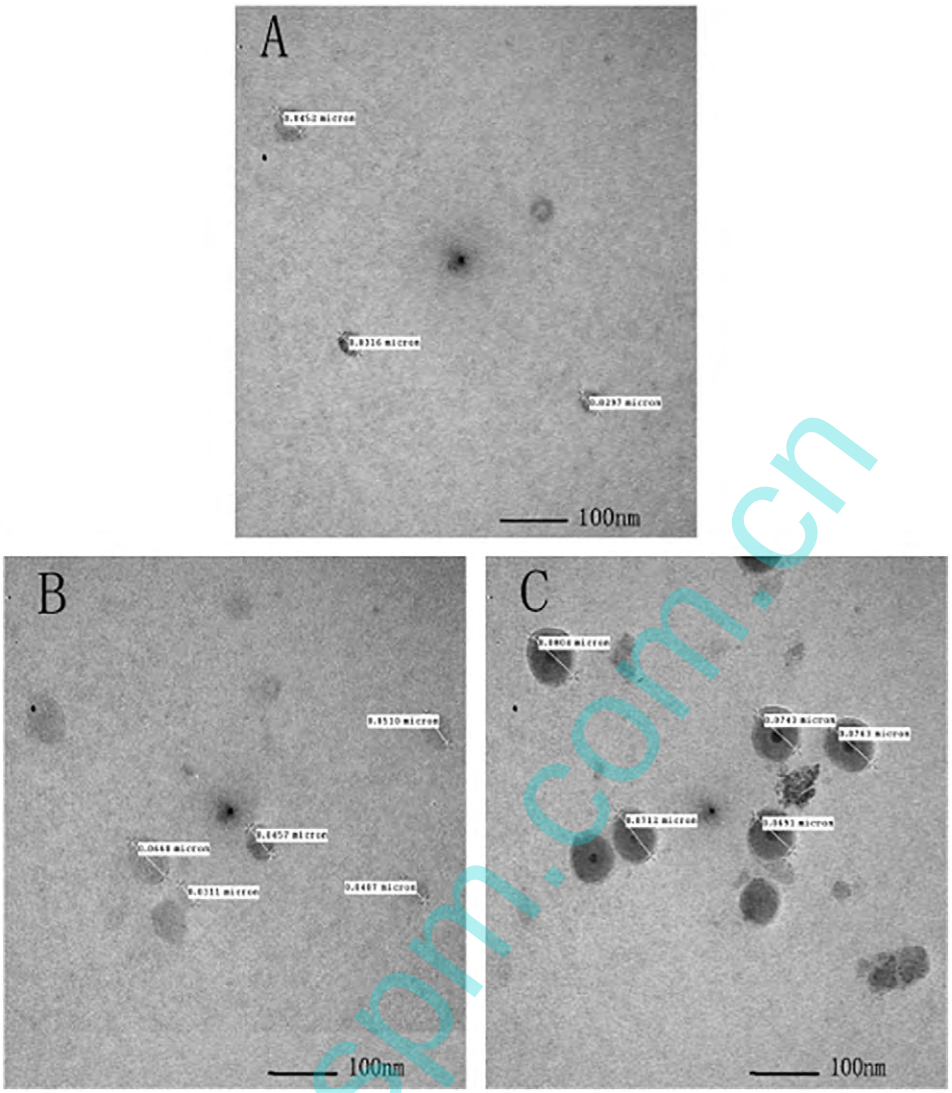

Fig. 2. APS/TEOS ratio for different size of silica particles:(A) APS/TEOS = 1/4, (B) APS/TEOS = 1/9, (C) APS/TEOS = 1/19.

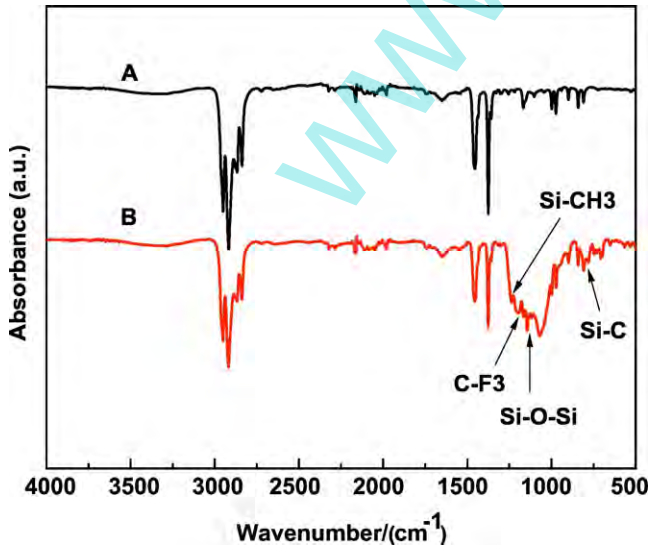

Fig. 3. FT-IR for the membranes. (A) Pure PP hollow fiber membrane (B) PP hollow fiber membrane after modification.

AFM image of the PP hollow fiber membranes are recorded for the roughness analyses of super-hydrophobic surface before and after modification with the silica particles. The surface roughness parameters are calculated using AFM. Table 2 presents the most important roughness parameters and their definitions [37]. An 8 μm × 8 μm surface was scanned. Over a length span of 4 μm, the RMS (Rq) roughness are 31.4 nm (Fig. 5A) and 49.5 nm (Fig. 5B), in addition the average roughness is 25.9 nm (Fig. 5A) and 38.7 nm (Fig. 5B), which indicate that the rough surface has been generated, and the surface has been superhydrophobicity.

The membrane was modified to incorporate chemically bonded silica particles as well as surface amine groups to the membrane for further hydrophobization. XPS is used to determine the surface composition of PP hollow fiber membranes that made from both silica particles and POTS. Although XPS cannot give a full account of the chemical composition for cotton textile samples due to their surface, it does provide qualitative information on the chemical changes before and after the modification [38]. It can be seen from Fig. 6A, in pure PP hollow fiber membrane, only the C and O peaks appeared in 285.02 eV and 532.2 eV. After being only modified by silica particles, there was a peak in 400.08, 154.2 and 103.1 eV which is attributed to N1s, Si2s, and Si2p signal (Fig. 6B), indicating the successful grafting of silica particles to the membrane. This is likely due to the formation of a 3D network layer. Further coated with silica particles and then modified with

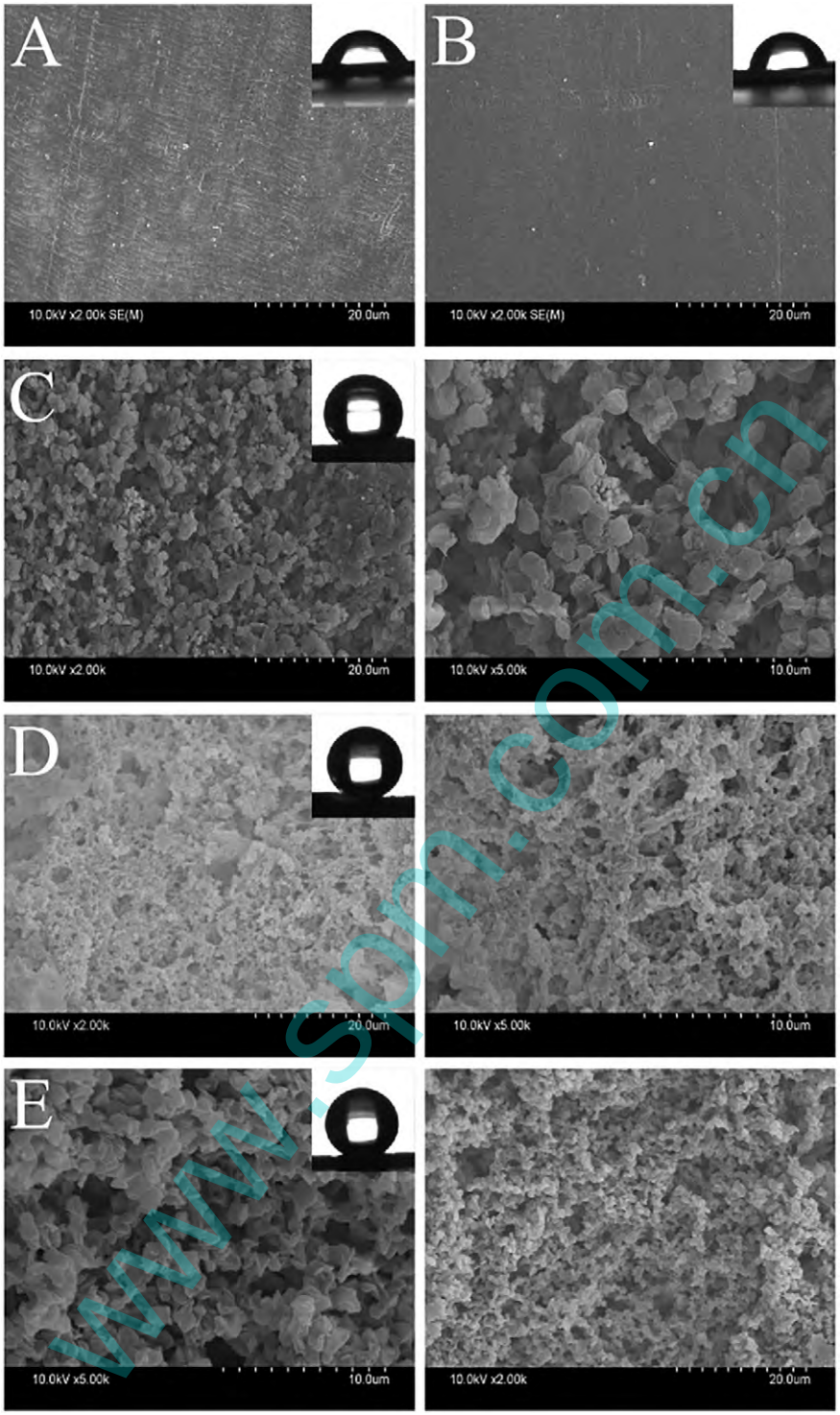

Fig. 4. SEM images for particle-covered PP Hollow fiber membranes. The images on the right are higher-magnification ones for those on the left. Shown in the insets are the images of static water droplets (5 μL) on the respective particle-covered membranes modified by POTS and silica particles. (A) pure PP membrane, (B) membrane modified only with POTS, (C) 1/19 silica particles covered, (D) 1/9 silica particles covered, (E) 1/4 silica particles covered.

POTS, signal due to Si2s, Si2p, C, O and F were observed (Fig. 6C), while the N1s peak disappeared completely. The free amine group was substituted by POTS. The observed Si/F/O/C ratio is 0.817/4.43/2.93/1. It suggests that a layer of POTS has covered the surface of the membrane. So the surface free energy of membrane was reduced. However, polypropylene particles may aggregate silica particles, therefore, the peak of Si2s, Si2p are low.

Average pore radius and interstitial porosity were determined by MIP. When the APS/TEOS ratios are 1/4, 1/9 and 1/19, the measured average pore radius increases (Fig. 7). The smallest average pore radius was 130 nm. This indicates that gas or liquid can freely through these porous, and the membrane and coating are not stoppage by silica particles. In this case, larger pores are more easily wetted than small ones. This means that large pores are first permeated by water, resulting in

Table 2
Roughness parameters and their definitions that can directly obtained by the use of AFM method [37].

Parameter	Definition
Arithmetic average height ($\bar{z}$)	General description of height variations
	$\bar{z}(N,M)=\frac{1}{N}\sum_{x=1}^{N} z(x,y)(2D)$
	$\bar{z}(N,M)=\frac{1}{MN}\sum_{x=1}^{N}\sum_{y=1}^{M} z(x,y)(3D)$
Average roughness (R_a)	Gives the deviation in height. Different profiles can give the same
	$R_a(N,M)=\frac{1}{N}\sum_{x=1}^{N}(z(x,y)-\bar{z}(N,M))(2D)$
	$R_a(N,M)=\frac{1}{NM}\sum_{x=1}^{N}\sum_{y=1}^{M}(z(x,y)-\bar{z}(N,M))(3D)$
Root-mean-square roughness (R_q)	Represents the standard deviation of surface heights
	$R_q(N,M)=\sqrt{\frac{1}{N}\sum_{x=1}^{N}(z(x,y)-\bar{z}(N,M))^2}(2D)$
	$R_q(N,M)=\sqrt{\frac{1}{NM}\sum_{x=1}^{N}\sum_{y=1}^{M}(z(x,y)-\bar{z}(N,M))^2}(3D)$

membrane contact angle decreases with larger pores. Meanwhile, when APS/TEOS ratio was 1/4, the interstitial porosity was 47.63%. As the porosity increase, the degrees of coating are small. Overall, there is little change. It appears that the membrane surface is porous after modification.

It can be seen from Fig. 8, when the silica particle content is 0.5 wt%, the surface coating is not uniform, and the roughness structure cannot effectively keep the air, water droplets can easily wet part of the membrane surface. So the contact angle is small, and the measurement error is also large. With the increase of silica content, the coating on the membrane surface is gradually distributed and stable, the membrane surface forms a micro-nano-rough structure. As the roughness of the surface

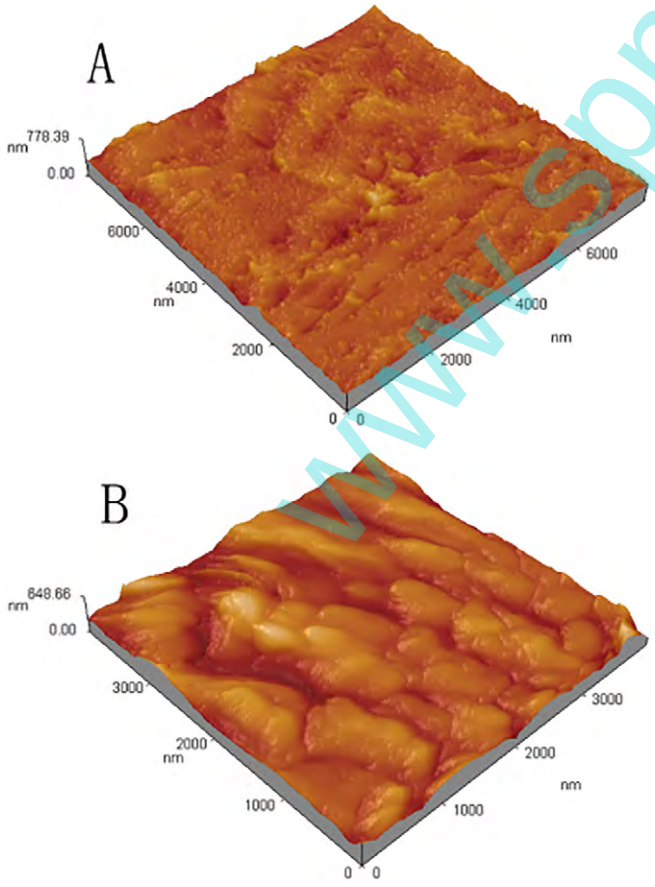

Fig. 5. AFM images for the PP Hollow fiber membranes. (A) pure PP membrane (B) PP membrane after modification with silica particles.

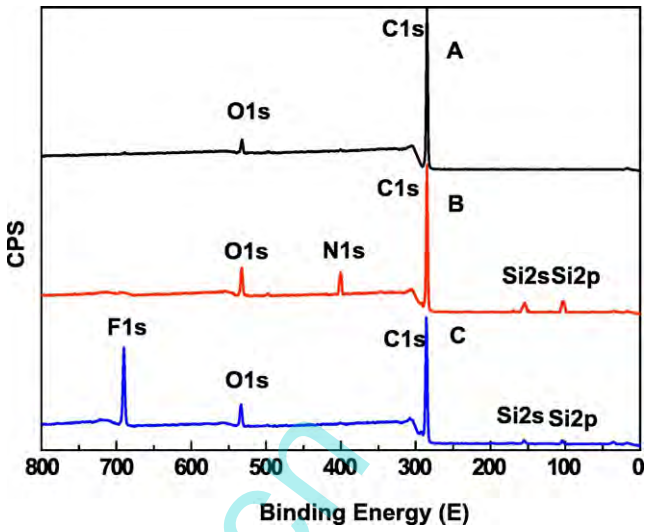

Fig. 6. XPS for the membranes: (A) pure PP hollow fiber membrane (B) PP hollow fiber membrane after modification silica particles (C) PP hollow fiber membrane after further modification with silica particles and POTS.

increases, the air is present on the rough surface. As a result, when the silica particle content increases from 1 wt% to 1.5 wt%, the contact angle increases and finally the super-hydrophobic membrane is obtained. However, with the increase of silica content to 2 wt%, the coating on the film surface is no longer stable, and many small particles aggregate to form large particles, meanwhile the coating structure becomes more smooth, which affects the micro-nano-roughness structure. So that the air layer decreases and the contact area between the water and the membrane surface increases, resulting in poor hydrophobicity of the membrane.

When the silica content is the same, the contact angles on the film are also different which different silica sols coats on the membranes. The smaller the size of the silica particles, the more pores are formed on the surface of the membrane and the more air is present in the pores of the membrane. Because of the smaller contact area of the water with the membrane surface, the contact angle increases. With the increase of silica particles, the pores are also increased, and the large pores are easily wetted by water droplets, so the contact angle of the membrane decreases because of the increase of the silica particles.

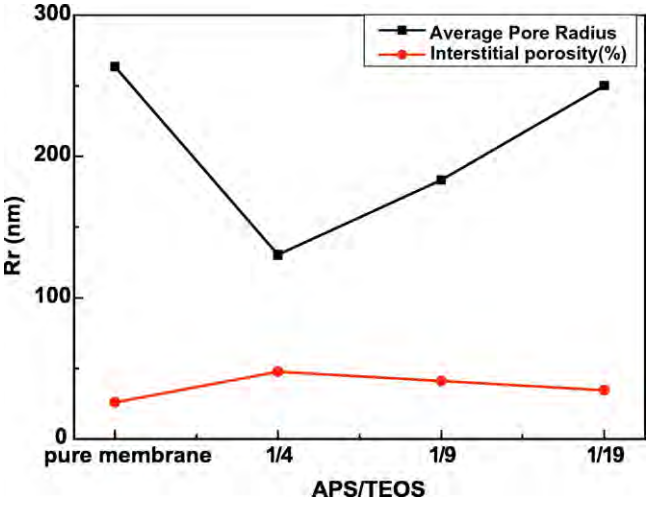

Fig. 7. Average pore radius and Interstitial porosity for different APS/TEOS ratio (The amount of silica is 1.5 wt%).

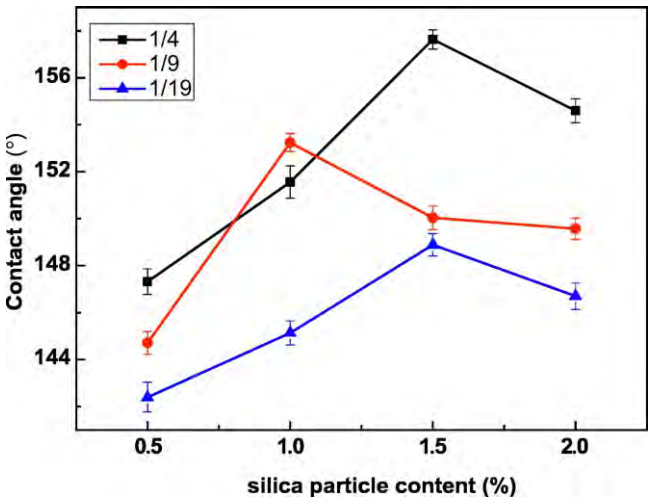

Fig. 8. The contact angle measurements under different content of silica particles.

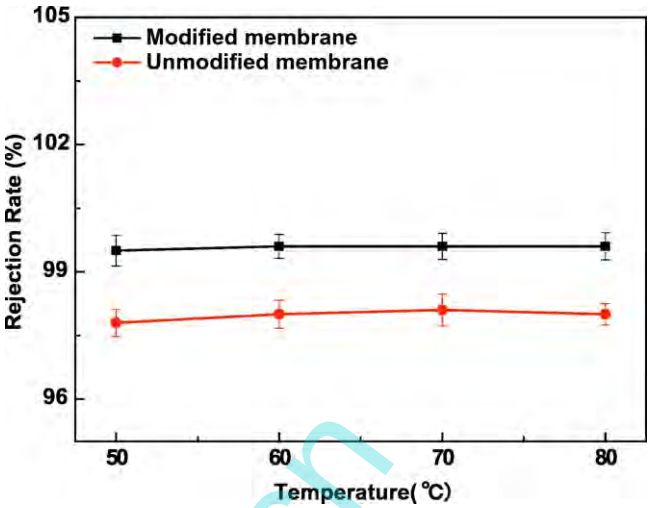

Fig. 10. Comparison with rejection rate of the unmodified membrane and modified membrane.

3.3. Comparison and analysis of membrane distillation

Membrane distillation is a membrane separation process, with the driving force being the vapor pressure difference between the two sides of the membrane. It can be seen from Fig. 9, when the temperature is constant, the flux increases with the hydrophobicity of the membrane. For Fig. 9A, this is because the membrane surface is a super-hydrophobic surface, so the NaCl solution cannot wet the membrane surface, and only the water vapor can through the membrane pores into the condensation side under pressure. While the NaCl macromolecules are trapped in the feed side. At the same time, this can increase the air gap between the liquid and the membrane surface, due to the roughness and high hydrophobicity of the super-hydrophobic membrane surface. And the water vapor through the membrane hole increases because of the membrane porosity (Fig. 7). It appeared that upon modification,the interstitial porosity slightly increased from 25.95 μm before modification to 47.63, 41.12 and 34.63 μm after modification by POTS, respectively. Due to the hydrophobicity of the B and C, the NaCl solution can be able to wet the membrane surface. In other words, the outer membrane pores are wetted and the majority of the membrane pores are dry, so the flux is slightly reduced, but large Molecular material is still not through the membrane hole. Fig. 9D is unmodified hollow fiber membrane, most of the membrane pores will be wetted by NaCl solution, and the raw material liquid through the membrane hole into the condensation side. On the other word, some of the biggest pores could be wetted and a limited transport of NaCl solution could occur [39]. Even some NaCl molecules may plug membrane pore to cause membrane pollution, resulting in membrane flux decline. As the hydrophobicity increases, the LEP increases [34,39,40]. LEP is defined as a pressure, at which liquid penetrates the pores and is transported through the hydrophobic membrane. But in some extreme cases, contaminants accumulate on the membrane surface that clogs the inlet of the cell, resulting in a large pressure drop. And it may even cause local pressure to exceed the LEP which cause leakage of the feedstock. However, the relation was nonlinear. In the same conditions, the flux of the membrane increases obviously at elevated feed temperature, which indicated that the saturated vapor pressure of the interfacial water increases with the increase of the feed temperature. An increase of feed temperature results in higher fluxes due to a higher driving force. Finally, the flux obviously increased.

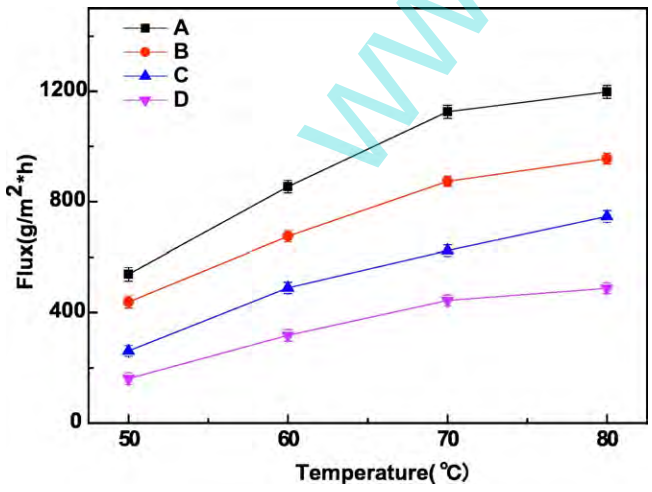

Fig. 9. MD permeateflux versus temperature for the different membranes. (A) APS/TEOS = 1/4, (B) APS/TEOS = 1/9, (C) APS/TEOS = 1/19, (D) unmodified membrane. Silica particle content is 1.5 wt%.

After the polypropylene hollow fiber membrane is modified into a super-hydrophobic membrane, the contact area between the membrane surface and the raw material liquid is reduced, so the contamination of the membrane surface is also reduced. And the macromolecules cannot pass through the membrane pores, the membrane can achieve better separation effect, the rejection rate of NaCl solution reaches 99.8%. The unmodified polypropylene hollow fiber membrane has poor hydrophobicity, and part of the NaCl solution could enter the condensation side through the membrane hole, so the rejection rate of the membrane to NaCl solution is 98%. The rejection is not affected by temperature (Fig. 10).

4. Conclusions

In summary, the obtained different sized silica particles as nanoparticles, MEK and cyclohexanone as a non-solvent are added to the sol. And polypropylene hollow fiber membranes are coated to form a rough coating. The amine groups are substituted by fluorosilane, which is attributed to reduce the surface free energy of the film. Finally, the super-hydrophobic hollow fiber membranes with contact angle of 157° were obtained. Due to the average pore radius are larger than 100 nm, air and brine can through porous. Simultaneously, the interstitial porosity indicates that the membrane is porous. The result of membrane distillation indicates that the modified membrane has higher flux than the untreated membrane, and the modified membrane has a higher retention rate than the untreated membrane. At the same time,

the flux of the membrane increases with increasing temperature, and the rejection does not change with increasing temperature.

Acknowledgments

The authors sincerely thank the National Basic Research Development Program of China (973 Program, 2012CB722706), National Natural Science Foundation of China (51273147), Specialized Research Fund for the Doctoral Program of Higher Education (20121201120002), The Science and Technology Plans of Tianjin (15PTSYJC00240) for financial support.

References

[1] R. Wang, K. Hashimoto, A. Fujishima, M. Chikuni, E. Kojima, A. Kitamura, M. Shimohigoshi, T. Watanabe, Light-induced amphiphilic surfaces, Nature (1997) 431–432.
[2] X. Gao, L. Jiang, Biophysics: water-repellent legs of water striders, Nature 432 (2004) 36.
[3] H. Kusumaatmaja, J.M. Yeomans, Anisotropic hysteresis on ratcheted superhydrophobic surfaces, Soft Matter 5 (2009) 2704.
[4] J. Seyfi, I. Hejazi, S.-H. Jafari, H.A. Khonakdar, G.M. Mohamad Sadeghi, A. Calvimontes, F. Simon, On the combined use of nanoparticles and a proper solvent/non-solvent system in preparation of superhydrophobic polymer coatings, Polymer 56 (2015) 358–367.
[5] L. Li, J. Tian, M. Li, W. Shen, Superhydrophobic surface supported bioassay—an application in blood typing, Colloids Surf. B: Biointerfaces 106 (2013) 176–180.
[6] T. Sun, H. Tan, D. Han, Q. Fu, L. Jiang, No platelet can adhere—largely improved blood compatibility on nanostructured superhydrophobic surfaces, Small 1 (2005) 959–963.
[7] N.J. Shirtcliffe, G. McHale, S. Atherton, M.I. Newton, An introduction to superhydrophobicity, Adv. Colloid Interf. Sci. 161 (2010) 124–138.
[8] T. Onda, S. Shibuichi, N. Satoh, K. Tsujii, Super-water-repellent fractal surfaces, Langmuir 12 (1996) 2125–2127.
[9] H.Y. Erbil, A.L. Demirel, Y. Avcı, O. Mert, Transformation of a simple plastic into a superhydrophobic surface, Science 299 (2003) 1377–1380.
[10] S. Shibuichi, T. Onda, N. Satoh, K. Tsujii, Super water-repellent surfaces resulting from fractal structure, J. Phys. Chem. 100 (1996) 19512–19517.
[11] S. Li, H. Li, X. Wang, Y. Song, Y. Liu, L. Jiang, D. Zhu, Super-hydrophobicity of large-area honeycomb-like aligned carbon nanotubes, J. Phys. Chem. B 106 (2002) 9274–9276.
[12] T. Sun, G. Wang, H. Liu, L. Feng, L. Jiang, D. Zhu, Control over the wettability of an aligned carbon nanotube film, J. Am. Chem. Soc. 125 (2003) 14996–14997.
[13] K.K.S. Lau, J. Bico, K.B.K. Teo, M. Chhowalla, G.A.J. Amaratunga, W.I. Milne, G.H. McKinley, K.K. Gleason, Superhydrophobic carbon nanotube forests, Nano Lett. 3 (2003) 1701–1705.
[14] Q. Xie, J. Xu, L. Feng, L. Jiang, W. Tang, X. Luo, C.C. Han, Facile creation of a super-amphiphobic coating surface with bionic microstructure, Adv. Mater. 16 (2004) 302–305.
[15] S. Grego, T.W. Jarvis, B.R. Stoner, J.S. Lewis, Template-directed assembly on an ordered microsphere Array, Langmuir 21 (2005) 4971–4975.
[16] M. Miwa, A. Nakajima, A. Fujishima, K. Hashimoto, T. Watanabe, Effects of the surface roughness on sliding angles of water droplets on superhydrophobic surfaces, Langmuir 16 (2000) 5754–5760.
[17] B. Zhao, W.J. Brittain, Synthesis of polystyrene brushes on silicate substrates via carbocationic polymerization from self-assembled monolayers, Macromolecules 33 (2000) 342–348.
[18] K.-H. Haas, S. Amberg-Schwab, K. Rose, Functionalized coating materials based on inorganic-organic polymers, Thin Solid Films 351 (1999) 198–203.
[19] C.M.A. Ershad-Langroudi, G. Vigier, R. Vassoille, Hydrophobic Hybrid Inorganic–organic Thin Film Prepared by Sol-gel Process for Glass Protection and Strengthening Applications, 1997.
[20] B. Mahltig, H. Böttcher, Modified silica sol coatings for water-repellent textiles, J. Sol-Gel Sci. Technol. 27 (2003) 43–52.
[21] Y. Lv, X. Yu, J. Jia, S.-T. Tu, J. Yan, E. Dahlquist, Fabrication and characterization of superhydrophobic polypropylene hollow fiber membranes for carbon dioxide absorption, Appl. Energy 90 (2012) 167–174.
[22] M. Yu, G. Gu, W.-D. Meng, F.-L. Qing, Superhydrophobic cotton fabric coating based on a complex layer of silica nanoparticles and perfluorooctylated quaternary ammonium silane coupling agent, Appl. Surf. Sci. 253 (2007) 3669–3673.
[23] R. Chouikh, S. Bouguecha, M. Dhahbi, Modelling of a modified air gap distillation membrane for the desalination of seawater, Desalination 181 (2005) 257–265.
[24] S. Al-Obaidani, E. Curcio, F. Macedonio, G. Di Profio, H. Al-Hinai, E. Drioli, Potential of membrane distillation in seawater desalination: thermal efficiency, sensitivity study and cost estimation, J. Membr. Sci. 323 (2008) 85–98.
[25] M.S. El-Bourawi, Z. Ding, R. Ma, M. Khayet, A framework for better understanding membrane distillation separation process, J. Membr. Sci. 285 (2006) 4–29.
[26] S.T. Hsu, K.T. Cheng, J.S. Chiou, Seawater desalination by direct contact membrane distillation, Desalination 143 (2002) 279–287.
[27] D. Singh, K.K. Sirkar, Desalination of brine and produced water by direct contact membrane distillation at high temperatures and pressures, J. Membr. Sci. 389 (2012) 380–388.
[28] A. El-Abbassi, A. Hafidi, M. Khayet, M.C. García-Payo, Integrated direct contact membrane distillation for olive mill wastewater treatment, Desalination 323 (2013) 31–38.
[29] A. El-Abbassi, A. Hafidi, M.C. García-Payo, M. Khayet, Engineering with Membranes 2008. Concentration of olive mill wastewater by membrane distillation for polyphenols recovery, Desalination 245 (2009) 670–674.
[30] S. Nene, S. Kaur, K. Sumod, B. Joshi, K.S.M.S. Raghavarao, Membrane distillation for the concentration of raw cane-sugar syrup and membrane clarified sugarcane juice, Desalination 147 (2002) 157–160.
[31] K. Christensen, R. Andresen, I. Tandskov, B. Norddahl, J.H. du Preez, Using direct contact membrane distillation for whey protein concentration, Desalination 200 (2006) 523–525.
[32] Á. Kozák, E. Békássy-Molnár, G. Vatai, The Third Membrane Science and Technology Conference of Visegrad Countries (PERMEA); part 2. Production of black-currant juice concentrate by using membrane distillation, Desalination 241 (2009) 309–314.
[33] Z. Jian, S. Bonyadi, T.S. Chung, Exploring the potential of commercial polyethylene membranes for desalination by membrane distillation, J. Membr. Sci. 497 (2015).
[34] J. Kujawa, S. Cerneaux, W. Kujawski, M. Bryjak, J. Kujawski, How to functionalize ceramics by perfluoroalkylsilanes for membrane separation process? Properties and application of hydrophobized ceramic membranes, ACS Appl. Mater. Interfaces 8 (2016) 7564–7577.
[35] H.F. Hoefnagels, D. Wu, G. de With, W. Ming, Biomimetic superhydrophobic and highly oleophobic cotton textiles, Langmuir 23 (2007) 13158–13163.
[36] I. Hejazi, J. Seyfi, E. Hejazi, G.M.M. Sadeghi, S.H. Jafari, H.A. Khonakdar, Investigating the role of surface micro/nano structure in cell adhesion behavior of superhydrophobic polypropylene/nanosilica surfaces, Colloids Surf. B: Biointerfaces 127 (2015) 233–240.
[37] M.M.A. Shirazi, D. Bastani, A. Kargari, M. Tabatabaei, Characterization of polymeric membranes for membrane distillation using atomic force microscopy, Desalin. Water Treat. 51 (2013) 6003–6008.
[38] E. Kontturi, P.C. Thüne, J.W. Niemantsverdriet, Cellulose model surfaces: simplified preparation by spin coating and characterization by X-ray photoelectron spectroscopy, infrared spectroscopy, and atomic force microscopy, Langmuir 19 (2003) 5735–5741.
[39] J. Kujawa, S. Cerneaux, S. Koter, W. Kujawski, Highly efficient hydrophobic titania ceramic membranes for water desalination, ACS Appl. Mater. Interfaces 6 (2014) 14223–14230.
[40] J. Kujawa, W. Kujawski, S. Koter, K. Jarzynka, A. Rozicka, K. Bajda, S. Cerneaux, M. Persin, A. Larbot, Membrane distillation properties of TiO2 ceramic membranes modified by perfluoroalkylsilanes, Desalin. Water Treat. 51 (2013) 1352–1361.